

End-Windings Modeling to Study Transient Voltage Distribution in Machine Stator Windings Using Finite Elements Method

R. S. Ferreira, A. C. Ferreira

Abstract— Many models to predict overvoltages in electrical machines due do steep-fronted surges use equivalent lumped circuit or multiconductor transmission line models. The knowledge of the electrical parameters used in these models is an important initial step do study transient overvoltages in electrical machine stator windings. To calculate the electrical parameters of the machine's end-windings region it is important to model all individual conductors and to consider strand and main insulations separately. In this context this work presents numerical simulations of the end-windings region of a large electrical machine by means of Finite Elements Method (FEM). Inductance and resistance are calculated, as a function of frequency, using an equivalent 2D geometry, being each strand modelled to take skin and proximity effects into account. Furthermore, regarding stray capacitances, the strand and main insulations are modelled and the extension of the semiconductive coating through the stator core is considered for calculating turn to ground capacitances by using the 3D geometry. The end-windings results are compared with those obtained for slot region to better understand the effects involved. Finally, the end-windings parameters are used in a model to predict coil to coil voltages when the machine is submitted to a steep-fronted voltage.

Keywords: electrical machines, transient overvoltages, Finite Elements Method (FEM), end-windings modeling.

I. INTRODUCTION

Electrical machines insulations are submitted to overvoltages during the normal operation. The knowledge of the amplitude and duration of these overvoltages are of great importance for the motor design. Normally the prediction of the overvoltages are obtained by using simulation models that require values of electrical parameters such as inductance, resistance and capacitance, for a wide range of frequency.

In general, the works found in the literature, normally, calculate electrical parameters to be used in the models to simulate the overvoltage distribution in electrical machines

windings by two different ways, analytically or by finite elements method (FEM).

Regarding high frequency electrical stator machine parameters, in [1] analytical equations are presented to obtain an equivalent lumped circuit. The main goal of the work is to study transient overvoltages in motor windings due to sequential pole closure. For inductance calculation, the equations consider slot and end-winding regions which consider the magnetic flux penetration in the stator core and in the air, respectively. Capacitances are calculated only for stator core region considering the conductors as parallel plates. Regarding end-windings region, the inductances are calculated as presented in [2] which have been defined using vector potential function by considering the coil as straight elements connected in series.

In [3] induction motor windings parameters are calculated using finite elements method by a 2D geometry as a function of frequency. The model takes into account skin and proximity effects and the magnetic flux penetration into stator core. The end-windings inductance is calculated approximating the real geometry by an axisymmetric half toroid.

Furthermore, in [4] the electrical parameters are calculated also using FEM in a 2D geometry. The parameters are calculated according to the rise time of the applied step voltage. For the simulations a lumped equivalent circuit which considers the slot and end-windings regions separated was considered.

Still using FEM simulations for a 2D geometry, in [5] the electrical parameters are calculated for a single coil for both sections, slot and end-windings. The model considers the magnetic walls for calculating parameters in slot region and an open boundary condition for end-windings region.

In this way the main goal of this paper is to calculate the electrical parameters, inductance, capacitance and resistance of end-windings region by means of FEM simulations based in a 3D geometry. The end-windings parameters are calculated as a function of frequency to be used in electromagnetic transient studies. A 3D model for the end-winding region for this kind of studies was not found in literature. The same parameters are also calculated for the slot region to be compared with those obtained for the end-windings region to better understand the effects involved. The end-windings parameters calculated are used in a model to simulate coil to coil transient voltage distribution when the line end coil of the machine is submitted to a steep-fronted voltage. Even having many works regarding the transient voltage distribution in electrical machines, a study that show the effect of the end-windings in the transient

This work was partially supported by INERGE (Instituto Nacional de Energia Elétrica), CNPq (Conselho Nacional de Desenvolvimento Científico e Tecnológico), CAPES (Coordenação de Aperfeiçoamento de Pessoal de Nível Superior) and FAPEMIG (Fundação de Amparo à Pesquisa do Estado de Minas Gerais).

R. S. Ferreira and A. C. Ferreira are with the Department of Electrical Engineering, Universidade Federal do Rio de Janeiro, COPPE/UFRJ, Rio de Janeiro, Brazil (e-mail: rodrigo.sousa@ufrj.br and ferreira@ufrj.br).

Paper submitted to the International Conference on Power Systems Transients (IPST2019) in Perpignan, France June 17-20, 2019.

results was not found. Therefore, using the modeling presented the influence of the end-windings region in the coil to coil voltages has been also verified.

II. MODELING

The model here presented considers the skin and proximity effects in the stranded conductors for both, slot and end-windings regions. Additionally, the magnetic barrier imposed by the stator core is also considered for the slot region.

In the next sections the slot region parameters are calculated using a 2D geometry and the end-windings parameters are obtained based in a 3D geometry.

The modeling and the numerical simulations are performed for a large motor (11 MW and 13.8 kV) which is normally not very common to be found in the literature.

A. End-Windings Modeling

To calculate the end-windings parameters correctly it is first necessary to draw the real geometry of the coil in this region. Fig. 1 shows the geometry of the end-winding modelled. For simulations only one coil has been considered, once the mutual effects with other coils can be neglected because the coupling between conductors of the same coil are much higher for high frequency studies [6].

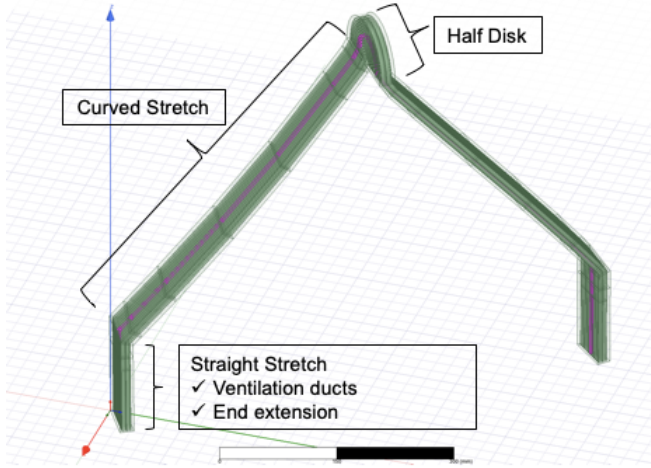


Fig. 1. 3D geometry of the end-winding modeled.

As can be seen in Fig. 1, by using a 3D geometry the correct shape of the coil can be modelled which is composed of straight, curved and half disk stretches. The curved stretch, which is larger for medium voltages than for low voltages machines [7], is defined by the coil pitch and the end-windings length. For the straight stretch the end extension of the coil in the stator core and the total length of the ventilation ducts present in stator were considered, since in these regions the coil is surrounded by air.

In Fig. 2 the cross section of the 3D coil is depicted. As can be seen, the coil is composed of main and strand insulations, and stranded conductors. The particular coil is formed by 13 turns and each turn has 2 strands. The first 6 strands are depicted in the figure by the nomenclature S_{X-Y} , where X is the turn and Y is the strand of the turn.

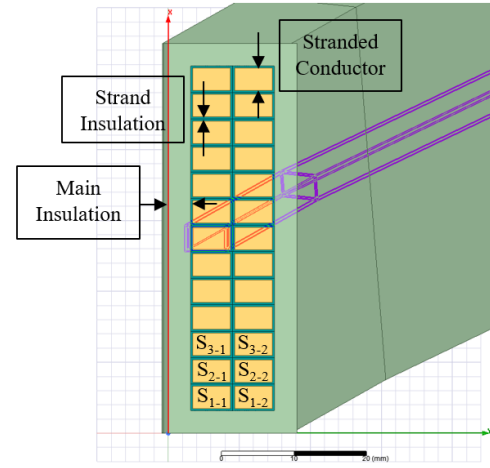


Fig. 2. Cross section of the 3D coil modeled.

1) Inductance and Resistance Calculation

To calculate the inductance and resistance it is necessary to model all stranded conductors individually, as the skin effect is only considered when solid conductors are modelled.

Resistance depends on frequency because at higher frequencies the current tends to flow near the surface of the conductor, as is well known as skin effect. In this context it is important to know the concept of penetration depth which can be calculated by:

$$\delta = \sqrt{2/(\omega \cdot \mu \cdot \sigma)} \quad (1)$$

where δ is the penetration depth in meters, ω is the angular frequency of the source of supply in rad/s, μ is the conductor's magnetic permeability in H/m and σ is the conductor's electric conductivity in S/m.

Moreover, resistance and inductance are dependent of the frequency due to the proximity effects in winding conductors, which can be explained by the result of circulating AC currents caused by magnetic fields generated by nearby conductors [8].

Inductance and resistance variation over frequency have been computed by an eddy current solver for a range of frequencies from 10 Hz to 10 MHz by applying the rated current in each conductor. To calculate inductance and resistance for high frequencies would be necessary extremely small mesh elements, once according to equation (1) the penetration depth is very small for frequencies in the range of MHz. Then using a 3D geometry for high frequencies becomes unpractical because of computation capabilities. In this way to calculate inductance and resistance for high frequencies a 2D equivalent model was used, based in the 3D original geometry. The 2D model is composed of two parts, the part 1 is modelled as a straight coil and corresponds to the straight and curved stretches depicted in Fig. 1. The part 2 is modelled as an axisymmetric geometry and corresponds to the half disk depicted in Fig. 1. The modeling has been validated by comparing the results obtained for rated frequency (60 Hz) for both models, 3D and the equivalent 2D, which presented good agreement.

Fig. 3 shows the magnetic field distribution for 60 Hz excitation using the 3D geometry.

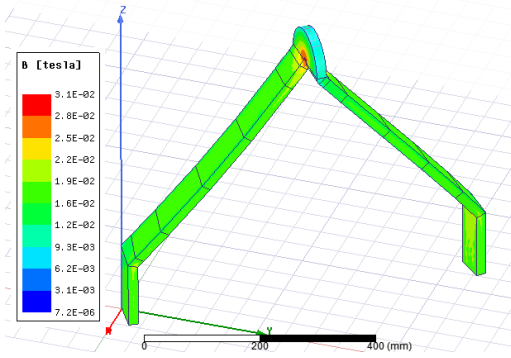


Fig. 3. Magnetic field distribution in the end-winding for 60 Hz excitation.

Moreover, in Fig. 4 the magnetic field is also presented for 60 Hz and 1 MHz, obtained from the 2D equivalent geometry. According to the figures the influence of the excitation frequency in the magnetic field distribution is clear. Still, to better visualize the effect of the high frequency in the field's distribution, Fig. 5 shows the current density distribution in the end-winding cross section for 10 MHz. Differently from the results obtained for 60 Hz, the current density distribution for 10 MHz is concentrated in a small thickness, as pointed out by the penetration depth equation, which means that it is not uniformly distributed in the conductor.

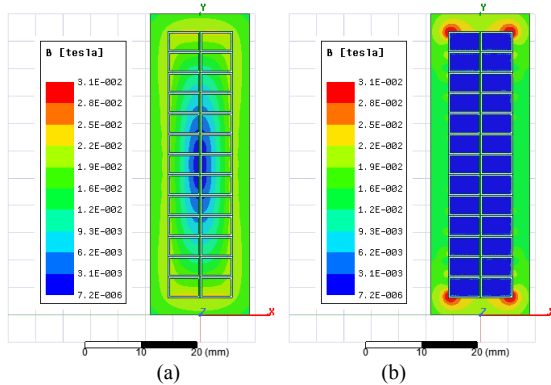


Fig. 4. Magnetic field distribution in the end-winding cross section for (a) 60 Hz and (b) 1 MHz.

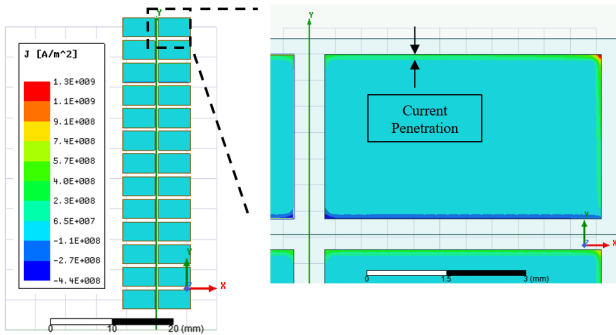


Fig. 5. Current density distribution in the end-winding cross section for 10 MHz.

Regarding the electrical parameters of each strand, Fig. 6 and Fig. 7 show the self and mutual resistances, respectively, and Fig. 8 and Fig. 9 show the self and mutual inductances, respectively, as a function of the simulated frequencies. The self-values are presented for the strand S_{1-1} , and the mutual values are between the strand S_{1-1} and the 5 first strands (S_{1-2}

... S_{3-2}), according to the nomenclature stated in Fig. 2. The values are normalized (in pu) in relation to the values of the self-resistance and self-inductance of the strand S_{1-1} for 60 Hz.

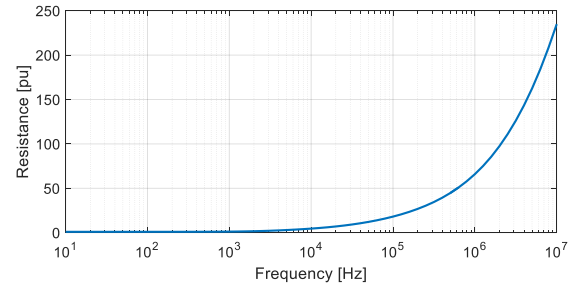


Fig. 6. End-winding self-resistance for strand S_{1-1} .

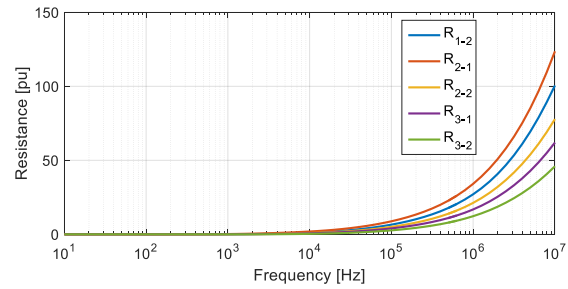


Fig. 7. End-winding mutual resistance in relation the strand S_{1-1} .

According to Fig. 6 and Fig. 7 the self and mutual resistances increase with the frequency as expected, due to skin and proximity effects. The main variation of the resistances occurs for frequencies higher than 10 kHz. Furthermore, regarding mutual resistance the highest value is observed for the strand S_{2-1} which is adjacent to the S_{1-1} strand in the "x" direction. For the inductance variation, according to Fig. 8 and Fig. 9 it can be noted that the values decrease with the frequency. This behavior is expected, once the magnetic flux lines inside the conductors is expelled from the stranded conductors for higher frequencies.

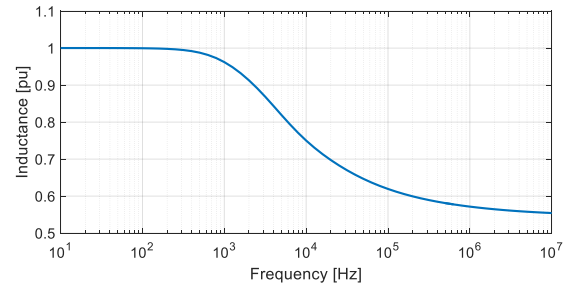


Fig. 8. End-winding self-inductance for strand S_{1-1} .

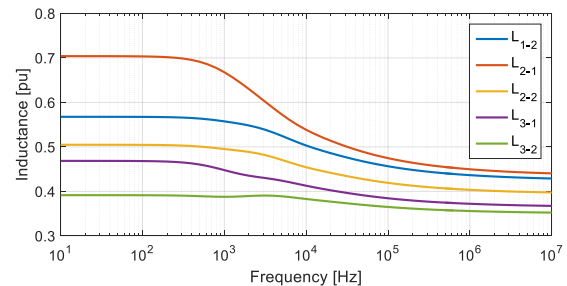


Fig. 9. End-winding mutual inductances in relation the strand S_{1-1} .

2) Capacitance Calculation

The capacitances have been calculated using the electrostatic solver from FEM. The model considers main and strand insulations modelled individually. The relative permittivities used in simulations are presented in TABLE I.

TABLE I
MAIN PARAMETERS USED IN ELECTROSTATIC SIMULATION.

| | |
|--------------------------------|-----|
| Strand insulation permittivity | 2.5 |
| Main insulation permittivity | 2.0 |

To obtain the results each turn is excited by a DC voltage, once the capacitances can be considered frequency independent. Turn to turn and turn to ground capacitances have been calculated by exciting the conductors with the expected voltage across each turn in normal operation. In the end-windings region the external surface of the coil cannot be considered totally grounded once there is no semiconductive coating in all this region. For the simulations it was considered that the semiconductive coating extends from the stator core by 10 mm. Furthermore, as aforementioned, the total length of the vent ducts was also considered in the 3D straight stretch, which is also grounded. Therefore, the grounded part of the end-windings region modelled is composed of the end extension of the coil in the stator core and the total length of the ventilation ducts. Fig. 10 and Fig. 11 show the voltage and electrical field distributions obtained for the end-windings region, respectively. Moreover, the same distributions on the coil cross section in the grounded part can be seen in Fig. 12. According to these figures it is possible to note in the grounded region of the 3D straight stretch that the voltage and the electric field are higher for the first turns than for the last turns of the coil.

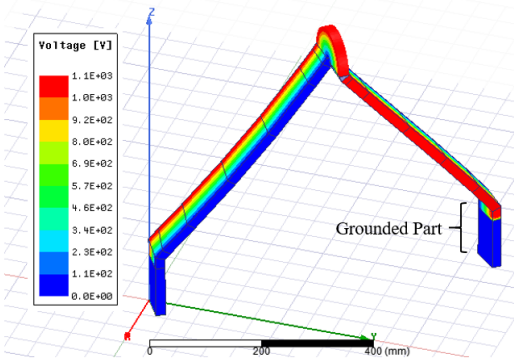


Fig. 10. Voltage distribution in the end-winding.

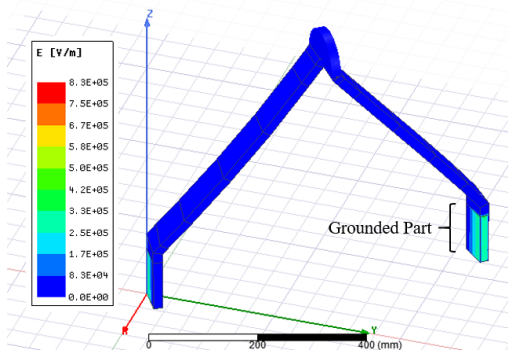


Fig. 11. Electrical field distribution in the end-winding.

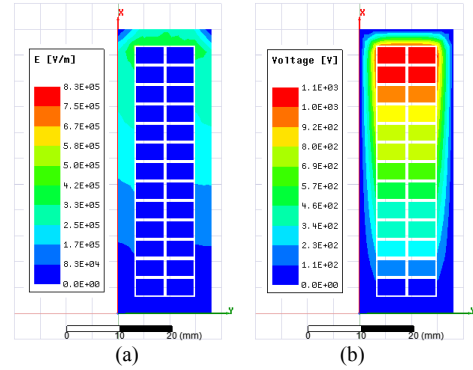


Fig. 12. (a) Electrical field and (b) voltage distributions in the end-winding cross section.

In TABLE II the numerical results obtained are presented. According to the simulations the capacitance of non-adjacent turns can be neglected.

TABLE II
CAPACITANCE VALUES FOR THE END-WINDINGS REGION.

| | | |
|---|---------------------------------------|-------|
| Mutual Capacitance of adjacent turns [pF] | | 450.3 |
| Turn to Ground Capacitances | First and Last Turns of the Coil [pF] | 23.8 |
| | Middle Turns of the Coil [pF] | 8.0 |

B. Slot Region Modeling

To verify the influence of the stator core, the electrical parameters are also calculated for the slot region and compared with the values obtained for the end-windings region.

Due to the symmetry in this region, the parameters are calculated using a 2D geometry for both solvers, electrostatic and eddy current. The model is comprised by a single coil in the slot region, using 1/84 of the complete geometry of the motor (the motor is formed by 84 coils) as can be seen in Fig. 13. The same nomenclature for the strands is used as showed in Fig. 2 for the end-windings region.

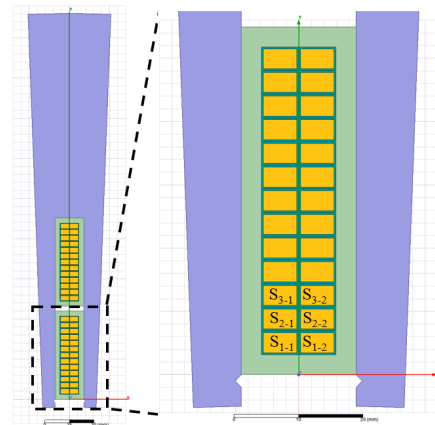


Fig. 13. Slot region geometry used in simulations.

In the next sub-sections, the electrical parameters calculated for the slot region are presented. The same methodology used to obtain the inductance, resistance and capacitance for end-windings region is used in slot region for both solvers, eddy current and electrostatic. For simulations only the conductors highlighted in Fig. 13 are excited.

1) Inductance and Resistance Calculation

Magnetic field flux lines for excitation of 60 Hz and 1 MHz can be seen in Fig. 14. As can be noted the magnetic core works as a barrier for high frequency excitations and the magnetic flux lines are concentrated in the main insulation region.

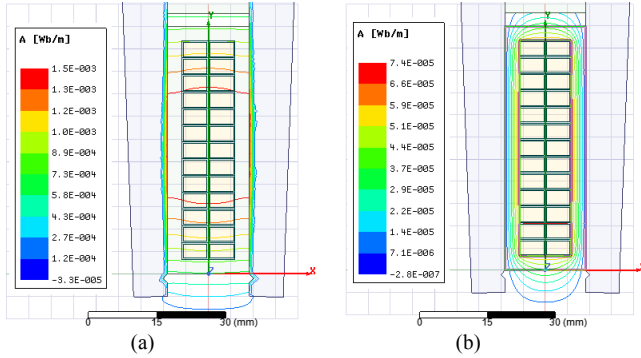


Fig. 14. Magnetic field flux lines for a) 60 Hz and b) 1 MHz.

Fig. 15 and Fig. 16 show the self and mutual resistances, respectively, and Fig. 17 and Fig. 18 show the self and mutual inductances, respectively, as a function of the simulated frequencies. In the same way the self-values are presented for the strand S_{1-1} , and the mutual values are between the strand S_{1-1} and the 5 first strands ($S_{1-2} \dots S_{3-2}$), according to the nomenclature stated in Fig. 13. The values are also normalized (in pu) in relation to the values of the self-resistance and self-inductance for 60 Hz in the slot region.

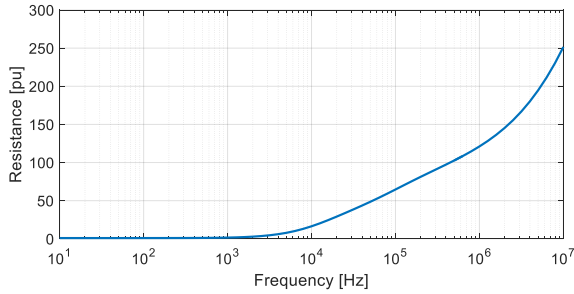


Fig. 15. Slot region self-resistance for strand S_{1-1} .

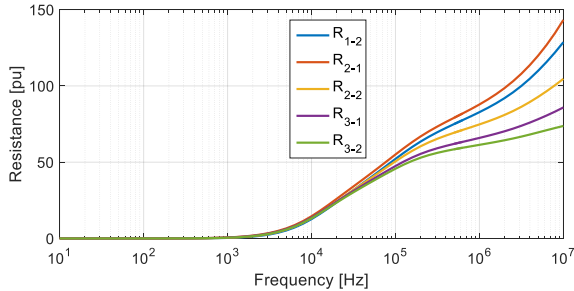


Fig. 16. Slot region mutual resistances for strand S_{1-1} .

According to the figures it is possible to note that the resistance and inductance in the stator core region are more affected than in the end-winding region, for both self and mutual values. Especially the inductance values are more affected when compared with the resistance values, because the stator core in high frequencies works as a barrier for the

magnetic flux lines.

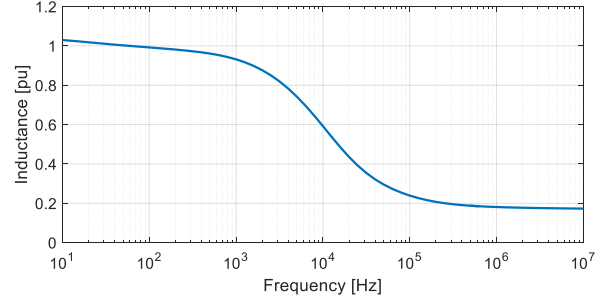


Fig. 17. Slot region self-inductance for strand S_{1-1} .

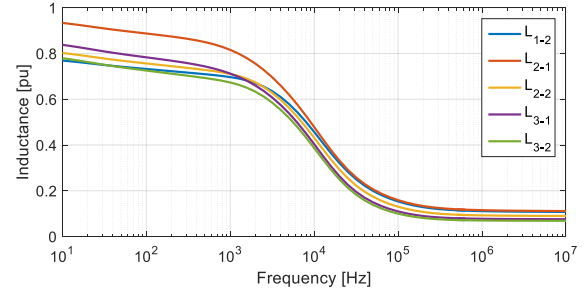


Fig. 18. Slot regions mutual inductances for strand S_{1-1} .

2) Capacitance Calculation

Capacitance values obtained are presented in TABLE III. The results of mutual capacitances are similar for both regions, although, the turn to ground capacitances are higher for slot region, as in this region the external surface of the coil is grounded in all extension of the core length.

TABLE III
CAPACITANCE VALUES FOR THE SLOT REGION.

| Mutual Capacitance of adjacent turns [pF] | | 879.4 |
|---|---------------------------------------|-------|
| Turn to Ground Capacitances | First and Last Turns of the Coil [pF] | 223.7 |
| | Middle Turns of the Coil [pF] | 75.8 |

III. TRANSIENT SIMULATIONS

In order to verify the influence of the end-windings the transient voltage distribution in the motor windings, the model presented in [9][10] has been used. The electrical equivalent circuit for the stator windings can be seen in Fig. 19, which shows in details one group of coils from phase “a”. Each stator turn is modeled as a “PI” section composed of elements in which transient magnetic fields are directly solved by finite elements method, identified by $L_1 \dots L_n$, and electric circuit elements which are related to the stray capacitances and end-windings parameters. The capacitances considered are the turn to turn ($C_{1-2} \dots C_{(n-1)-n}$) and the turn to ground (C_n), which represent the sum of the values obtained for end-windings and slot regions. Resistance and inductance of end-windings for each individual conductor ($R_{ew1} \dots R_{ewn}$ and $L_{ew1} \dots L_{ewn}$, respectively) are considered as calculated in the previous sections according to the dominant frequency of the applied voltage. The surge is applied in the line end coil of group 1 from phase “a” and the line end coils of phases “b” and “c” and the other coil groups are grounded (the motor is composed of 4 coil groups).

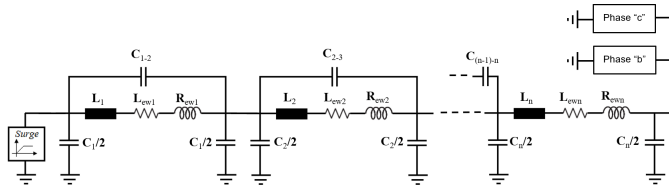


Fig. 19. Equivalent circuit for stator winding for transient simulation.

The simulations have been performed for a surge of 100 V with a rise time of 1 μ s. To verify the influence of end-windings region the results obtained considering the lumped parameters (Case 1) are compared with those when the end-windings influence is neglected (Case 2). Fig. 20 and Fig. 21 show the coil to coil voltage and the peak voltage, respectively, for the seven coils of one group of coils.

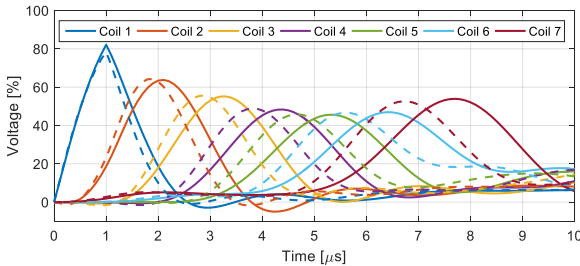


Fig. 20. Coil to coil transient voltage distribution (Case 1: solid lines and Case 2: dashed lines).

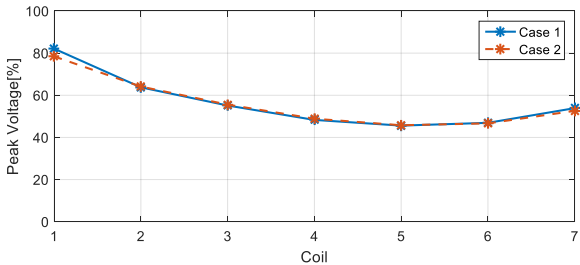


Fig. 21. Peak voltage across each coil.

As can be seen in the previous figures the first coil is the one submitted to the highest overvoltage and the end-windings parameters has minimum influence in the voltage peak and more influence in the waveforms. The small variation of peak voltages is explained by the curves showed in the previous sections, where the variation for slot region is higher than in end-windings region. The main difference observed in the waveforms is due to the additional end-windings stray capacitances considered in Case 1.

IV. CONCLUSIONS

In this paper the electrical parameters used to simulate the transient voltage distribution in stator winding machines are calculated in the end-windings region. Normally, these parameters are calculated analytically or by using FEM in a simplified 2D geometry.

Resistance and inductance have been calculated considering proximity and skin effects in the strand conductor using an equivalent 2D model for high frequencies. Turn to turn and turn to ground capacitances were calculated considering that the end-windings surface is grounded in just a

portion of the straight stretch of the overhang, by using a 3D geometry, as in real medium voltage machines. The same parameters are also calculated for the slot region to be compared with those obtained for the end-windings region.

It was observed, for self and mutual values, that the resistances increase, and the inductances decrease with the increasing of the frequency for the end-windings region. The same relation has been found in the slot region, for both inductance and resistance values, however the effect is more pronounced due to the flux barrier imposed by the stator core for the high frequencies excitations.

The values calculated in the end-windings region have been used to obtain the transient coil to coil voltage. The results using lumped parameters calculated for the surge dominant frequency and neglecting them have been compared. According to the results, the transient voltage distribution, indeed, depends on the end-windings parameters, nevertheless, only a small influence in the peak voltages has been observed, once the high frequency affects more the slot region. For the waveform results it was observed a higher influence of the end-windings stray capacitances.

The end-windings parameters calculated will be used to obtain the transient voltage distribution between turns and from turns to ground in a future work.

V. REFERENCES

- [1] J. L. Guardado and K. J. Cornick, "Calculation of machine winding electrical parameters at high frequencies for switching transient studies," in *IEEE Transactions on Energy Conversion*, vol. 11, no. 1, pp. 33-40, March 1996.
- [2] P. J. Lawrenson, "Calculation of machine end-winding inductances with special reference to turbogenerators," in *Proceedings of the Institution of Electrical Engineers*, vol. 117, no. 6, pp. 1129-1134, June 1970.
- [3] V. Venegas, J. L. Guardado, E. Melgoza and M. Hernandez, "A Finite Element Approach for the Calculation of Electrical Machine Parameters at High Frequencies," *2007 IEEE Power Engineering Society General Meeting*, Tampa, FL, 2007, pp. 1-5.
- [4] A. Krings, G. Paulsson, F. Sahlén and B. Holmgren, "Experimental investigation of the voltage distribution in form wound windings of large AC machines due to fast transients," *2016 XXII International Conference on Electrical Machines (ICEM)*, Lausanne, 2016, pp. 1700-1706.
- [5] M. K. Ussain and P. Gomez, "Modeling and Experimental Analysis of the Transient Overvoltages on Machine Windings Fed by PWM Inverters," *International Conference on Power Systems Transients (IPST2017)*, Seoul, 2017.
- [6] M. T. Wright, S. J. Yang and K. McLeay, "General theory of fast-fronted interturn voltage distribution in electrical machine windings," in *IEE Proceedings B - Electric Power Applications*, vol. 130, no. 4, pp. 245-256, July 1983.
- [7] G. Stone, E. A. Boulter, I. Culbert and H. Dhirani, *Electrical Insulation for Rotating Machines: Design, Evaluation, Aging, Testing, and Repair*, 2nd Edition, Wiley-IEEE Press, 2014.
- [8] R. Wrobel, A. Mlot and P. H. Mellor, "Investigation of end-winding proximity losses in electromagnetic devices," *The XIX International Conference on Electrical Machines - ICEM 2010*, Rome, 2010, pp. 1-6.
- [9] R. S. Ferreira and A. C. Ferreira, "Transient Voltage Distribution in Induction Motor Stator Windings Using Finite Elements Method," *International 44th Annual Conference of the IEEE Industrial Electronics Society*, Washington, 2018.
- [10] W. N. Fu, P. Zhou, D. Lin, S. Stanton and Z. J. Cendes, "Modeling of solid conductors in two-dimensional transient finite-element analysis and its application to electric machines" in *IEEE Transactions on Magnetics*, vol. 40, no. 2, pp. 426-434, March 2004.